

Strong-coupling functional renormalization group: Nagaoka ferromagnetism and non-Fermi liquid physics in the Hubbard model at $U = \infty$

Jonas Arnold, Peter Kopietz, and Andreas Rückriegel

*Institut für Theoretische Physik, Universität Frankfurt,
Max-von-Laue Straße 1, 60438 Frankfurt, Germany*

(Dated: December 17, 2025)

We develop an extension of the fermionic functional renormalization group for systems where strong correlations give rise to projected Hilbert spaces. We use our method to calculate the phase diagram and the electronic spectral function of the Hubbard model at infinite on-site repulsion where many-body states involving doubly occupied lattice sites are eliminated from the physical Hilbert space. For a square lattice with nearest-neighbor hopping we find that the ground state evolves from a paramagnetic Fermi liquid at low densities via a state with antiferromagnetic stripe order at intermediate densities to an extended Nagaoka ferromagnet at high densities. In the strongly correlated magnetic phases, the electrons form an incoherent non-Fermi liquid. Both at high and low densities, the volume of the Fermi surface is not constrained by Luttinger's theorem.

Introduction.—Strongly correlated electrons are of central interest in modern condensed matter physics. In spite of many decades of intense research, fundamental questions in this field remain open due a lack of controlled methods for dealing with strong interactions in dimensions larger than one. The predictive power of numerical approaches is limited by the exponentially growing dimension the Hilbert space with the system size, while analytical methods often suffer from uncontrolled or biased approximations. A notable exception is the fermionic functional renormalization group (FRG) [1–6] which in the past 25 years has been established as an unbiased theoretical tool for detecting instabilities of interacting electrons on a lattice for weak to intermediate strength of the interaction [7–20]. Unfortunately, in the strong-coupling regime the inevitable truncations of the formally exact FRG flow equations break down so that up until now it has not been possible to apply FRG methods to models for correlated electrons in the regime where the interaction is much larger than any other energy scale. In this work, we use our recently developed [21] formulation of the FRG in terms of Hubbard X-operators [22–24] dubbed X-FRG to transcend this limitation.

In the extremely correlated regime [25–27] many-body states involving doubly occupied lattice sites are excluded from the low-energy Hilbert space of the Hubbard model. The effective Hamiltonian in the low-energy sector is the t - J model [22, 28] which is believed to describe key features in the normal state of high-temperature cuprate superconductors. The Hilbert space projection is believed to play an important role for a number of exotic properties, such as a pseudogap in the electronic spectral function and a disjoined Fermi surface made up of Fermi arcs which has been observed both in cuprates [29–34] and in optical lattices [35, 36]. The list of exotic strong-coupling phenomena includes also the violation of Luttinger's theorem [21, 37–42] (i.e., the volume enclosed by the Fermi surface is not related to the total electronic density), and kinetic Nagaoka ferromagnetism which is

subject to continuous theoretical investigations [43–67] and has recently been realized experimentally in optical lattices [68, 69]. In fact, as pointed out by Anderson [70–72], to understand the effect of the Hilbert space projection on the single-particle excitations it is sufficient to consider the t - J model in the limit $J \rightarrow 0$, which is equivalent to the limit of infinite on-site repulsion $U \rightarrow \infty$ in the Hubbard model. The Hamiltonian is then given by the projected kinetic energy

$$\mathcal{H} = \sum_{ij} \sum_{\sigma} t_{ij} h_{i\sigma}^{\dagger} h_{j\sigma} - \mu \sum_i \sum_{\sigma} n_{i\sigma}, \quad (1)$$

where the holon operators $h_{i\sigma}$ and $h_{i\sigma}^{\dagger}$ act on the projected Hilbert space consisting of fermionic Fock states without doubly occupied lattice sites. In this space $h_{i\sigma}$ and $h_{i\sigma}^{\dagger}$ annihilate and create a spin- σ electron at site i , while $n_{i\sigma} = h_{i\sigma}^{\dagger} h_{i\sigma}$ counts the number of spin- σ electrons in a grand canonical ensemble with chemical potential μ . Despite its simple quadratic form, the Hamiltonian (1) is highly non-trivial because $h_{i\sigma}$ creates a hole in a restricted Hilbert space without double occupancy. As a consequence, $h_{i\sigma}$ and $h_{i\sigma}^{\dagger}$ are *not* canonical fermion operators but obey the non-canonical anticommutation relations

$$h_{i\sigma} h_{j\sigma'}^{\dagger} + h_{j\sigma'}^{\dagger} h_{i\sigma} = \delta_{ij} [\delta_{\sigma\sigma'} (1 - n_{i\bar{\sigma}}) + \delta_{\sigma\bar{\sigma}'} h_{i\bar{\sigma}}^{\dagger} h_{i\sigma}], \quad (2)$$

where $\bar{\sigma} = -\sigma$. The relation (2) encodes the restricted local Hilbert space, and in particular entails the constraint $n_{i\uparrow} + n_{i\downarrow} = 0$ or 1 . In the rest of this work we will refer to the Hamiltonian (1) as the t model. For simplicity we assume nearest neighbor hopping on a square lattice, i.e. $t_{ij} = t$ for all pairs i, j of nearest neighbors and $t_{ij} = 0$ otherwise.

The X-FRG [21] extends the spin FRG proposed in Ref. [73] (for recent applications see Refs. [74 and 75]) to more general models for strongly correlated electrons. The basic idea of the X-FRG is to use a non-trivial local deformation of the original model as initial condition

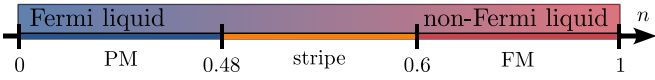


FIG. 1. Ground state phase diagram of the t model. With increasing density n , the system transitions from a paramagnet (PM) to stripe magnet to ferromagnet (FM). This is accompanied by a crossover from a Fermi liquid at small n to an incoherent non-Fermi liquid at large n .

for the FRG flow [76–78]. The flow equations provide an unbiased and non-perturbative resummation of non-local correlations which allows us to apply the full power of the established FRG machinery [4–6, 79, 80] to lattice models defined on restricted Hilbert spaces. By identifying the dominant instabilities of the X-FRG flow, we are able to map out the phase diagram of the t model shown in Fig. 1. In agreement with most earlier studies, we find an extended kinetic or Nagaoka ferromagnet phase at high densities [46, 47, 50, 52, 55, 57, 60–63, 65, 67] that is separated from a low-density paramagnet by an intermediate antiferromagnetic stripe state. Moreover, the X-FRG gives momentum-resolved access to the electronic spectral function, revealing that with increasing density, the t model gradually transitions from a conventional Fermi liquid to an incoherent non-Fermi liquid [61, 81, 82], and that Luttinger’s theorem [37–39] is broken in the restricted Hilbert space [21, 40–42].

X-FRG for the t model.—The X-FRG sets out from the exactly solvable $t = 0$ limit of isolated Hubbard atoms. Hopping-induced correlation effects are incorporated by a non-perturbative resummation of the high-temperature series in t/T . This is achieved by replacing $t \rightarrow t_\Lambda = \Lambda t$ and following the evolution of the effective holon action from $\Lambda = 0$ to 1, which is equivalent to lowering the temperature from infinity to $T = 1/\beta$ [74, 83]. The starting point is the generating functional of imaginary-time-ordered connected holon correlation functions,

$$e^{\mathcal{G}_\Lambda[\bar{j}, j]} = \text{Tr} \left\{ e^{\beta \mu_0 \sum_{i\sigma} n_{i\sigma} \mathcal{T} e^{-\int_0^\beta d\tau \sum_{i,j\sigma} t_{\Lambda,ij} h_{i\sigma}^\dagger(\tau) h_{j\sigma}(\tau)}} \right. \\ \left. \times e^{\int_0^\beta d\tau \sum_{i\sigma} [\delta\mu_\Lambda h_{i\sigma}^\dagger(\tau) h_{i\sigma}(\tau) + \bar{j}_{i\sigma}(\tau) h_{i\sigma}(\tau) + h_{i\sigma}^\dagger(\tau) j_{i\sigma}(\tau)]} \right\}, \quad (3)$$

where $h_{i\sigma}(\tau) = e^{\mu_0 \tau} h_{i\sigma}$, \mathcal{T} denotes imaginary-time ordering, and $j_{i\sigma}(\tau)$ and $\bar{j}_{i\sigma}(\tau)$ are Grassmann source fields. Note that we also include a counter-term $\delta\mu_\Lambda$ for the chemical potential. Hence, $\mu = \mu_0 + \delta\mu_\Lambda$, with the Hubbard atom initial value $\mu_0 = T \ln[n/(2-2n)]$ for a given density n . The counter-term allows us to keep the density n fixed as Λ varies; this is advantageous because n controls the high-frequency behavior of the holon propagator (4).

In Ref. [21], we have shown that $\mathcal{G}_\Lambda[\bar{j}, j]$ satisfies a standard fermionic FRG flow equation. Hence, we can use it to apply the established machinery of the fermionic FRG [4, 5] to the t model (1). To that end, we parametrize

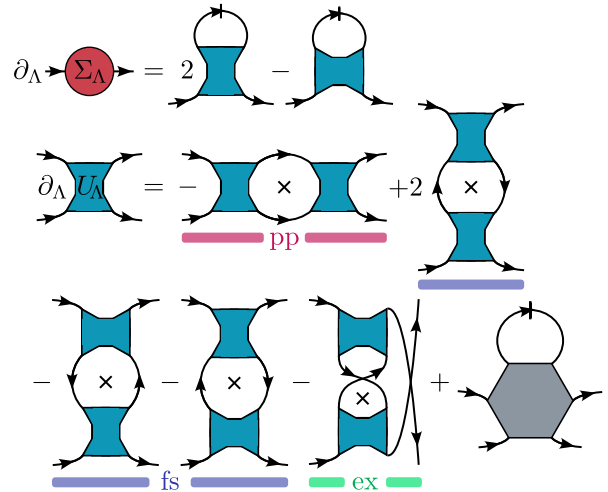


FIG. 2. Graphical representation of the flow equations for (a) holon self-energy $\Sigma_\Lambda(K)$ and (b) two-body interaction vertex $U_\Lambda(K'_1, K'_2; K_2, K_1)$. Lines with arrows denote the holon propagator $G_\Lambda(K)$. An additional dash means the single-scale propagator $\dot{G}_\Lambda(K) = G_\Lambda^2(K) \partial_\Lambda(t_{\Lambda,k} - 2\delta\mu_\Lambda/3)$. Crosses inside loops signify that each $G_\Lambda(K)$ is subsequently replaced by $\dot{G}_\Lambda(K)$.

the holon propagator as [21, 83]

$$G_\Lambda(K) = \frac{Z}{i\omega + \mu_0 - Z(t_{\Lambda,k} - 2\delta\mu_\Lambda/3) - Z\Sigma_\Lambda(K)}, \quad (4)$$

where $K = (\mathbf{k}, \omega)$ collects crystal momentum \mathbf{k} and fermionic Matsubara frequency ω , the quasi-particle residue of the Hubbard atom is $Z = 1 - n/2$, and the holon self-energy $\Sigma_\Lambda(K)$ encodes effects of t_Λ beyond tree-level. Its flow is governed by the two-body interaction vertex $U_\Lambda(K'_1, K'_2; K_2, K_1)$, which is itself determined by the particle-particle (pp), forward-scattering (fs), and exchange (ex) ladder diagrams and the three-body interaction vertex, which we neglect. See Fig. 2 for a graphical representation of the relevant flow equations. Following the methodology of fermionic FRG, we apply a channel decomposition [5, 11, 15] to the two-body interaction,

$$U_\Lambda(K'_1, K'_2; K_2, K_1) = \mathcal{V}(\omega_2, \omega_1) - \mathcal{S}_\Lambda(Q_{\text{pp}}; \omega'_2, \omega_1) + \mathcal{M}_\Lambda(Q_{\text{ex}}; \omega_2, \omega_1) \\ + \frac{1}{2} [\mathcal{M}_\Lambda(Q_{\text{fs}}; \omega_1, \omega_2) - \mathcal{C}_\Lambda(Q_{\text{fs}}; \omega_2, \omega_1)]. \quad (5)$$

Here, \mathcal{S}_Λ , \mathcal{M}_Λ , and \mathcal{C}_Λ are the superconducting, magnetic, and charge channels, respectively, $Q_x = (\mathbf{q}_x, \Omega_x)$, $x \in \{\text{pp}, \text{fs}, \text{ex}\}$ denote the relevant (bosonic) momentum-frequency transfers, and \mathcal{V} is a Q_x -independent part of the Hubbard atom vertex. Due to the holon algebra (2),

the channels have non-trivial initial conditions,

$$Z^2 \mathcal{V}(\omega_2, \omega_1) = -G_0^{-1}(\omega_2) - G_0^{-1}(\omega_1), \quad (6a)$$

$$Z^2 \mathcal{M}_0(\Omega; \omega_2, \omega_1) = \beta \delta_{\Omega,0} \frac{n}{2} G_0^{-1}(\omega_2) G_0^{-1}(\omega_1), \quad (6b)$$

$$Z^2 \mathcal{C}_0(\Omega; \omega_2, \omega_1) = \beta \delta_{\Omega,0} \frac{n}{2} (1-n) G_0^{-1}(\omega_2) G_0^{-1}(\omega_1), \quad (6c)$$

and $\mathcal{S}_0 = 0$, where $G_0(\omega) = Z/(i\omega + \mu_0)$ is the propagator of the Hubbard atom. As both \mathcal{M}_0 and \mathcal{C}_0 are finite and singular, any single-channel truncation of the X-FRG flow is bound to miss important physics of the projected Hilbert space. Therefore we keep all three channels. To detect possible ordering instabilities, it is however sufficient to retain only the most singular contribution to the flow in each channel [11]. In this approximation, the channel flow equations subject to the Hubbard atom initial conditions (6) can still be solved analytically. Furthermore, we heuristically incorporate a part of the neglected diagram involving the three-body vertex via a Katanin substitution [84]. However, because of the non-trivial initial frequency dependence in Eq. (6), the Katanin substitution treats two-loop corrections to U_Λ inconsistently. This is remedied by also approximating $G_0^{-1}(\omega) G_\Lambda(K) \approx 1 + (t_{\Lambda,\mathbf{k}} - 2\delta\mu_\Lambda/3) G_\Lambda(K)$ in internal loops. Details of the solution of the flow equations are presented in the companion paper [83]. In the rest of this work, we showcase the main features of the phase diagram and the spectral function of the square lattice t model that is generated by the X-FRG flow. To that end, we solved the flow equations for $\Sigma_\Lambda(K)$ and $\delta\mu_\Lambda$ numerically on a grid with 190 \mathbf{k} -points in the irreducible wedge of the Brillouin zone and 100 positive Matsubara frequencies.

Magnetic instabilities.—Both superconducting and charge channels remain relatively featureless and at most $\mathcal{O}(t)$ throughout the entire parameter space [83]. In contrast, the magnetic channel, shown in Fig. 3 for a representative selection of n and T , develops pronounced instabilities for $n \gtrsim 0.48$ at low temperatures: For $0.48 \lesssim n \lesssim 0.59$ the system favors a stripe phase with ordering vector $\mathbf{q} = (\pi, 0)$. This is consistent with the best known variational wavefunctions for the Nagaoka state [50, 55], which become unstable at a critical hole doping because the gap of a $(\pi, 0)$ spin wave vanishes. At $0.6 \lesssim n \lesssim 1$ on the other hand, the dominant instability is towards the kinetic (Nagaoka) ferromagnet with $\mathbf{q} = (0, 0)$, in agreement with Monte Carlo [60] and density-matrix renormalization group results [63, 65]. In these works, the ferromagnet is at first only partially polarized and becomes fully polarized at higher densities close to the variational estimates [50, 52, 55]. Since we only observe a ferromagnetic instability, we cannot distinguish between these two cases [85]. Note that the magnetic instabilities shift to higher temperatures as the density is increased. We attribute this to the increas-

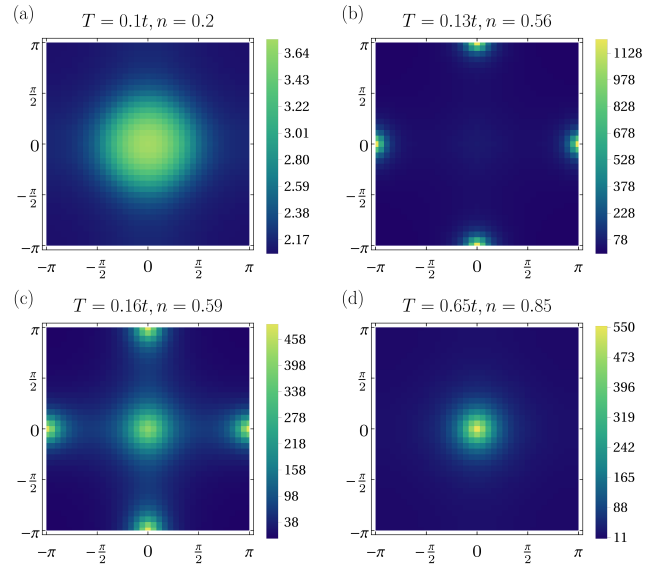


FIG. 3. Brillouin zone plots of the static part of the magnetic channel $M_{\Lambda=1}(\mathbf{q}, 0; 0, 0)/t$. (a) $n = 0.2$, $T = 0.14t$ in the paramagnetic state; (b) $n = 0.56$, $T = 0.13t$ showing the stripe instability; (c) $n = 0.59$, $T = 0.16t$ where stripe and ferromagnetic instabilities compete; and (d) $n = 0.85$, $T = 0.64t$ showing the instability towards the Nagaoka ferromagnet.

ing importance of the kinematic interaction due to the restricted Hilbert space with increasing n . Shortly after encountering the magnetic instabilities, the exponentially growing fluctuations lead to a breakdown of the numerics. Also, for $n \gtrsim 0.99$, our truncation is apparently insufficient to deal with the strong kinematic interactions, preventing us from accessing the regime $T \lesssim t$ and observing any kind of instability.

Spectral properties.—Since our X-FRG flow gives us access to the full holon self-energy $\Sigma_\Lambda(K)$, we can also address the electronic spectral properties of the t model in the entire phase diagram. To that end, we analytically continue the holon propagator (4) to real frequencies and compute the spectral function

$$A(\mathbf{k}, \omega) = -\frac{1}{\pi} \text{Im}[G_{\Lambda=1}(\mathbf{k}, \omega)|_{i\omega \rightarrow \omega + i\eta}]. \quad (7)$$

For the numerical analytical continuation, we use Padé approximants [86, 87] with $\eta = 0.001t$. In the paramagnetic phase at low densities shown in Fig. 4(a), we generally find a washed out band with sharp excitations around the Fermi edge, indicating a Fermi liquid. In contrast, at the magnetic instabilities at larger densities and low temperatures, shown in Fig. 4(b) and (c) for the stripe and kinetic ferromagnet, respectively, the spectral function becomes increasingly incoherent [61, 81, 82]. With growing n , the band becomes both narrower and significantly smeared out, with spectral weight transferred away from the Fermi edge into a negative-energy continuum that extends between the \mathbf{X} and \mathbf{M} points.

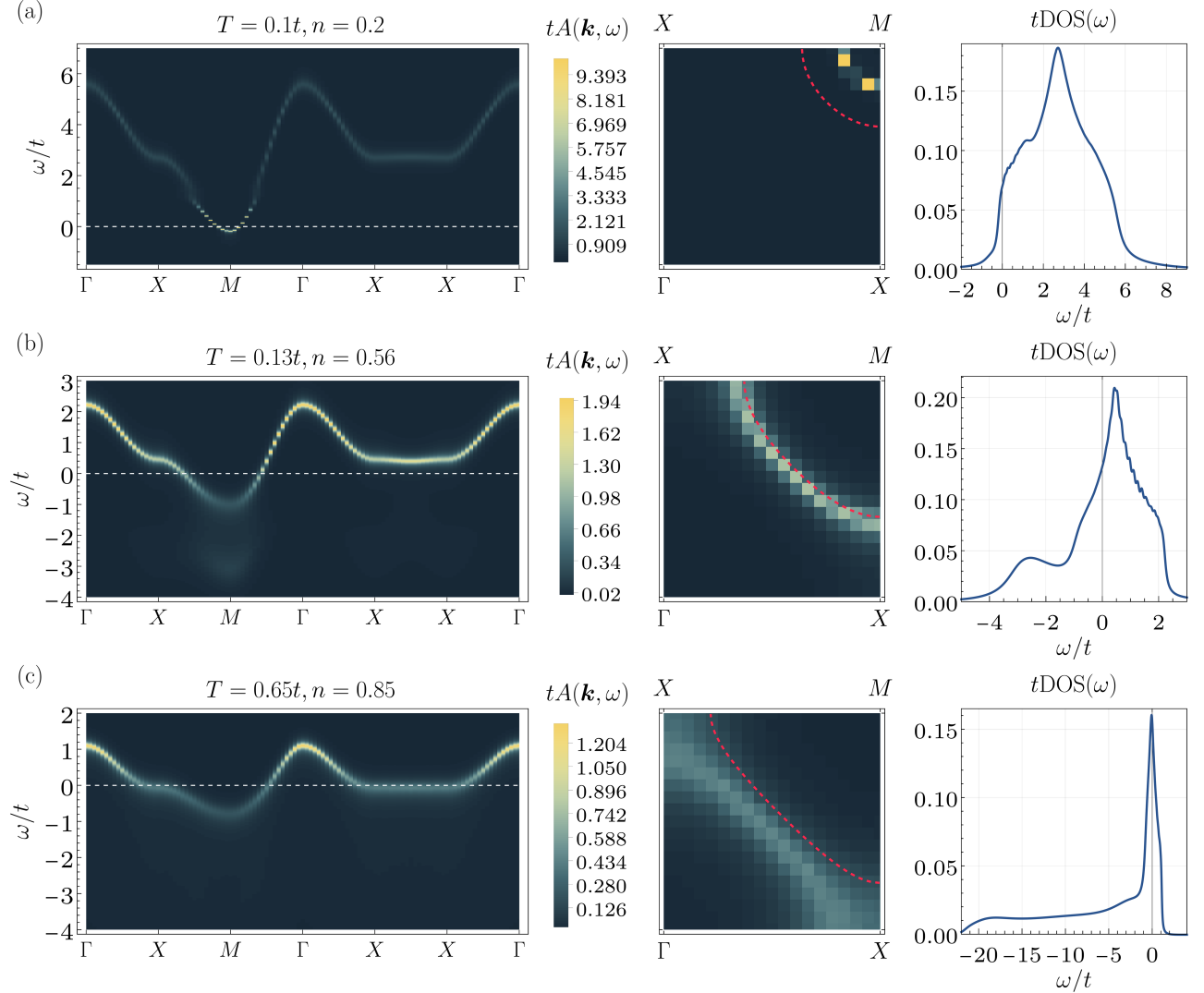


FIG. 4. Electronic spectral properties for (a) $n = 0.2$ and $T = 0.14t$ in the paramagnet, (b) $n = 0.56$ and $T = 0.13t$ coinciding with the stripe instability, and (c) $n = 0.85$ and $T = 0.65t$ where the system is unstable towards kinetic ferromagnetism. From left to right: Spectral function $tA(\mathbf{k}, \omega)$ along a high-symmetry path through the Brillouin zone, with the dashed line marking the Fermi energy; $tA(\mathbf{k}, 0)$ defining the Fermi surface, with the dashed red line indicating the Fermi surface of free electrons with the same n for comparison; the density of states $tDOS(\omega) = (1/N) \sum_{\mathbf{k}} tA(\mathbf{k}, \omega)$. For $n = 0.2$, we regularized the DOS with $\eta = 0.1t$ because in this case the quasi-particle peaks at the Fermi surface are sharper than our \mathbf{k} -resolution.

As the Fermi energy no longer hosts well-defined quasi-particles, the system is a non-Fermi liquid in this case. The marked asymmetry between particle- and hole-like excitations that develops for large n can be understood in terms of the Hilbert space projection: While for a particle, there are few states available to scatter into because most sites are occupied, there are many scattering states for a hole. In consequence, the latter are less coherent than the former [82]. A detailed analysis of the bandwidth, quasi-particle residues and damping as function of n and T will be presented in the companion paper [83]. Note also that similar to other examples of correlation-induced ferromagnetism [88–93], the ferromagnetic instability coincides with the Fermi energy ap-

proaching the van-Hove singularity of the narrow band. Last, from Fig. 4 it is also obvious that both at small and large n Luttinger’s theorem [37–39] is violated [21, 40–42]. Luttinger’s theorem is approximately satisfied only in the intermediate regime exhibiting the stripe instability where $\mu \approx 0$ [83, 94].

Conclusions.—In this work we have reported on an FRG calculation of the phase diagram and electronic spectral properties of the t model, i.e., the Hubbard model at $U = \infty$. By combining the recently developed X-FRG approach [21] with the established FRG machinery for canonical fermions, we have identified both a paramagnetic Fermi liquid at low densities and an incoherent non-Fermi liquid at higher densities, which displays both

antiferromagnetic stripe and kinetic ferromagnetic instabilities. The latter emerges only at high densities, in agreement with previous works [46, 47, 50, 52, 55, 57, 60–63, 65, 67], and coincides with a van-Hove singularity close to the Fermi edge. These results showcase that the X-FRG is a powerful tool for the investigation of strongly correlated systems with restricted Hilbert spaces. Since it is formally based on a high-temperature expansion, the X-FRG approach is unbiased. By solving the X-FRG flow, a diagrammatic resummation of the high-temperature series to infinite orders is obtained, which gives access to the low-temperature physics as well. Moreover, unlike most numerical approaches, the X-FRG works directly in the thermodynamic limit. Hence, it is not plagued by finite-size effects [60, 64]. It is also straightforward to improve upon our truncation along the lines established for fermionic FRG [14–20]. In future work, the X-FRG approach could be extended to more general lattices and interactions, as well as to more realistic models such as the t - J model [21]. Moreover, the lineshapes shown in Fig. 4 can be useful to understand future experiments probing the spectral functions in extremely strongly correlated electronic systems realized in optical lattices [68, 69].

This work was financially supported by the Deutsche Forschungsgemeinschaft (DFG, German Research Foundation) through Project No. 431190042.

- [10] M. Ossadnik, C. Honerkamp, T. M. Rice, and M. Sigrist, *Breakdown of Landau Theory in Overdoped Cuprates near the Onset of Superconductivity*, Phys. Rev. Lett. **101**, 256405 (2008).
- [11] C. Husemann and M. Salmhofer, *Efficient parametrization of the vertex function, Ω scheme, and the t, t' Hubbard model at van Hove filling*, Phys. Rev. B **79**, 195125 (2009).
- [12] C. Husemann, K.-U. Giering, and M. Salmhofer, *Frequency-dependent vertex functions of the (t, t') Hubbard model at weak coupling*, Phys. Rev. B **85**, 075121 (2012).
- [13] C. Taranto, S. Andergassen, J. Bauer, K. Held, A. Katanin, W. Metzner, G. Rohringer, and A. Toschi, *From Infinite to Two Dimensions through the Functional Renormalization Group*, Phys. Rev. Lett. **112**, 196402 (2014).
- [14] J. Lichtenstein, D. S. de la Peña, D. Rohe, E. D. Napoli, C. Honerkamp, and S. A. Maier, *High-performance functional Renormalization group calculations for interacting fermions*, Computer Physics Communications **213**, 100 (2017).
- [15] D. Vilardi, C. Taranto, and W. Metzner, *Nonseparable frequency dependence of the two-particle vertex in interacting fermion systems*, Phys. Rev. B **96**, 235110 (2017).
- [16] C. Honerkamp, *Efficient vertex parametrization for the constrained functional renormalization group for effective low-energy interactions in multiband systems*, Phys. Rev. B **98**, 155132 (2018).
- [17] D. Vilardi, C. Taranto, and W. Metzner, *Antiferromagnetic and d -wave paring correlations in the strongly interacting two-dimensional Hubbard model from the functional renormalization group*, Phys. Rev. B **99**, 104501 (2019).
- [18] J. Ehrlich and C. Honerkamp, *Functional renormalization group for fermion lattice models in three dimensions: Application to the Hubbard model on the cubic lattice*, Phys. Rev. B **102**, 195108 (2020).
- [19] C. Hille, F. B. Kugler, C. J. Eckhardt, Y.-Y. He, A. Kauch, C. Honerkamp, A. Toschi, and S. Andergassen, *Quantitative functional renormalization group description of the two-dimensional Hubbard model*, Phys. Rev. Res. **2**, 033372 (2020).
- [20] C. Honerkamp, D. M. Kennes, V. Meden, M. M. Scherer, and R. Thomale, *Recent developments in the functional renormalization group approach to correlated electron systems*, Eur. Phys. J. B **95**, 205 (2022).
- [21] A. Rückriegel, J. Arnold, R. Krämer, and P. Kopietz, *Functional renormalization group without functional integrals: Implementing Hilbert space projections for strongly correlated electrons via Hubbard X-operators*, Phys. Rev. B **108**, 115104 (2023).
- [22] P. Fulde, *Electron Correlations in Molecules and Solids*, (Springer, Berlin, Third Enlarged Edition, 1995).
- [23] Y. A. Izyumov and Y. N. Skryabin, *Statistical Mechanics of Magnetically Ordered Systems*, (Springer, Berlin, 1988).
- [24] S. G. Ovchinnikov and V. V. Val'kov, *Hubbard Operators in the Theory of Strongly Correlated Electrons*, (Imperial College Press, London, 2004).
- [25] B. S. Shastry, *Extremely correlated quantum liquids*, Phys. Rev. B **81**, 045121 (2010).
- [26] B. S. Shastry, *Extremely correlated Fermi liquids*, Phys. Rev. Lett. **107**, 056403 (2011).

- [27] B. S. Shastry, *Extremely correlated Fermi liquids: The formalism*, Phys. Rev. B **87**, 125124 (2013).
- [28] P. Fazekas, *Lecture Notes on Electron Correlation and Magnetism*, (World Scientific, Singapore, 1999).
- [29] D. S. Dessau, Z.-X. Shen, D. M. King, D. S. Marshall, L. W. Lombardo, P. H. Dickinson, A. G. Loeser, J. DiCarlo, C.-H. Park, A. Kapitulnik, and W. E. Spicer, *Key features in the measured band structure of $\text{Bi}_2\text{Sr}_2\text{CaCu}_2\text{O}_{8+\delta}$: Flat bands at E_F and Fermi surface nesting*, Phys. Rev. Lett. **71**, 2781 (1993).
- [30] M. R. Norman, H. Ding, M. Randeria, J. C. Campuzano, T. Yokoya, T. Takeuchi, T. Takahashi, T. Mochiku, K. Kadowaki, P. Guptasarma, and D. G. Hinks, *Destruction of the Fermi surface in underdoped high- T_c superconductors*, Nature **392**, 157-160 (1998).
- [31] K. M. Shen, F. Ronning, D. H. Lu, F. Baumberger, N. J. C. Ingle, W. S. Lee, W. Mevesana, Y. Kohsaka, M. Azuma, M. Takano, H. Takagi, and Z.-X. Shen, *Nodal Quasiparticles and Antinodal Charge Ordering in $\text{Ca}_{2-x}\text{Na}_x\text{CuO}_2\text{Cl}_2$* , Science **307**, 901-904 (2005).
- [32] A. Kanigel, U. Chatterjee, M. Randeria, M. R. Norman, S. Souma, M. Shi1, Z. Z. Li, H. Raffy, and J. C. Campuzano, *Protected Nodes and the Collapse of Fermi Arcs in High- T_c Cuprate Superconductors*, Phys. Rev. Lett. **99**, 157001 (2007).
- [33] H.-B. Yang, J. D. Rameau, Z.-H. Pan, G. D. Gu, P. D. Johnson, H. Claus, D. G. Hinks, and T. E. Kidd, *Reconstructed Fermi Surface of Underdoped $\text{Bi}_2\text{Sr}_2\text{CaCu}_2\text{O}_{8+\delta}$ Cuprate Superconductors*, Phys. Rev. Lett. **107**, 047003 (2011).
- [34] F. C. Zhang and T. M. Rice, *Effective Hamiltonian for the superconducting Cu oxides*, Phys. Rev. B **37**, 3759(R) (1988).
- [35] A. Bohrdt, L. Homeier, C. Reinmoser, E. Demler, F. Grusdt, *Exploration of doped quantum magnets with ultracold atoms*, Annals of Physics, **435**, 168651 (2021).
- [36] L. H. Kendrick, A. Kale, Y. Gang, A. D. Deters, M. Lebrat, A. W. Young, M. Greiner, *Pseudogap in a Fermi-Hubbard quantum simulator*, arXiv:2509.18075.
- [37] J. M. Luttinger, *Fermi Surface and Some Simple Equilibrium Properties of a System of Interacting Fermions*, Phys. Rev. **119**, 1153 (1960).
- [38] M. Oshikawa, *Topological Approach to Luttinger's Theorem and the Fermi Surface of a Kondo Lattice*, Phys. Rev. Lett. **84**, 3370 (2000).
- [39] K. Seki and S. Yunoki, *Topological interpretation of the Luttinger theorem*, Phys. Rev. B **96**, 085124 (2017).
- [40] W. Stephan and P. Horsch, *Fermi surface and dynamics of the t-J model at moderate doping*, Phys. Rev. Lett. **66**, 2258 (1991).
- [41] W. O. Putikka, M. U. Luchini, and R. R. P. Singh, *Violation of Luttinger's Theorem in the Two-Dimensional t-J Model*, Phys. Rev. Lett. **81**, 2966 (1998).
- [42] J. Kokalj and P. Prelovšek, *Luttinger sum rule for finite systems of correlated electrons*, Phys. Rev. B **75**, 045111 (2007).
- [43] Y. Nagaoka, *Ground state of correlated electrons in a narrow almost half-filled s-band*, Solid State Commun. **3**, 409 (1965).
- [44] Y. Nagaoka, *Ferromagnetism in a Narrow, Almost Half-Filled s Band*, Phys. Rev. **147**, 392 (1966).
- [45] L. M. Roth, *Spin wave stability of the ferromagnetic state for a narrow s-band*, Journal of Physics and Chemistry of Solids, **28**, 1549-1555 (1967).
- [46] B. S. Shastry, H. R. Krishnamurthy, and P. W. Anderson, *Instability of the Nagaoka ferromagnetic state of the $U = \infty$ Hubbard model*, Phys. Rev. B **41**, 2375 (1990).
- [47] Yu. A. Izyumov and B. M. Letfulov, *A diagram technique for Hubbard operators: the magnetic phase diagram in the (t-J) model*, J. Phys.: Condens. Matter **2** 8905 (1990).
- [48] A. G. Basile and V. Elser, *Stability of the ferromagnetic state with respect to a single spin flip: Variational calculations for the $U=\infty$ Hubbard model on the square lattice*, Phys. Rev. B **41**, 4842(R) (1990).
- [49] M. Kotrla and V. Drchal, *Mean-Field Solution of Strongly Correlated Systems Using Hubbard Atomic Operators*, phys. stat. sol. (b) **167**, 635 (1990).
- [50] W. von der Linden and D. M. Edwards, *Ferromagnetism in the Hubbard model*, J. Phys.: Condens. Matter **3**, 4917 (1991).
- [51] W. O. Putikka, M. U. Luchini, and M. Ogata, *Ferromagnetism in the two-dimensional t-J model*, Phys. Rev. Lett. **69**, 2288 (1992).
- [52] Th. Hanisch and E. Müller-Hartmann, *Ferromagnetism in the Hubbard model: instability of the Nagaoka state on the square lattice*, Ann. Physik **2**, 381 (1993).
- [53] G. Chiappe, E. Louis, J. Gala'n, F. Guinea, and J. A. Verge's, *Ground-state properties of the $U=\infty$ Hubbard model on a 4×4 cluster*, Phys. Rev. B **48**, 16539 (1993).
- [54] M. W. Long and X. Zotos, *Hole-hole correlations in the $U = \infty$ limit of the Hubbard model and the stability of the Nagaoka state*, Phys. Rev. B **48**, 317 (1993).
- [55] P. Wurth and E. Müller-Hartmann, *Ferromagnetism in the Hubbard model: Spin waves and instability of the Nagaoka state*, Ann. Phys. **507**, 144 (1995).
- [56] M. Kollar, R. Strack, and D. Vollhardt, *Ferromagnetism in correlated electron systems: Generalization of Nagaoka's theorem*, Phys. Rev. B **53**, 9225 (1996).
- [57] T. Obermeier, T. Pruschke, and J. Keller, *Ferromagnetism in the large- U Hubbard model*, Phys. Rev. B **56**, R8479(R) (1997).
- [58] E. V. Kuz'min, *The ground state problem in the infinite- U Hubbard model*, Phys. Solid State **39**, 169-178 (1997).
- [59] H. Tasaki, *From Nagaoka's Ferromagnetism to Flat-Band Ferromagnetism and Beyond*, Prog. Theor. Phys. **99**, 489 (1998).
- [60] F. Becca and S. Sorella, *Nagaoka Ferromagnetism in the Two-Dimensional Infinite- U Hubbard Model*, Phys. Rev. Lett. **86**, 3396 (2001).
- [61] H. Park, K. Haule, C. A. Marianetti, and G. Kotliar, *Dynamical mean-field theory study of Nagaoka ferromagnetism*, Phys. Rev. B **77**, 035107 (2008).
- [62] G. Carleo, S. Moroni, F. Becca, and S. Baroni, *Itinerant ferromagnetic phase of the Hubbard model*, Phys. Rev. B **83**, 060411(R) (2011).
- [63] L. Liu, H. Yao, E. Berg, S. R. White, and S. A. Kivelson, *Phases of the Infinite U Hubbard Model on Square Lattices*, Phys. Rev. Lett. **108**, 126406 (2012).
- [64] I. Ivantsov, A. Ferraz, and E. Kochetov, *Breakdown of the Nagaoka phase at finite doping*, Phys. Rev. B **95**, 155115 (2017).
- [65] G. G. Blesio, M. G. Gonzalez, and F. T. Lisandrini, *Magnetic phase diagram of the infinite- U Hubbard model with nearest- and next-nearest-neighbor hoppings*, Phys. Rev. B **99**, 174411 (2019).
- [66] R. Samajdar and R. N. Bhatt, *Polaronic mechanism of Nagaoka ferromagnetism in Hubbard models*, Phys. Rev. B **109**, 235128 (2024).

- [67] R. C. Newby and E. Khatami, *Finite-temperature kinetic ferromagnetism in the square-lattice Hubbard model*, Phys. Rev. B **111**, 245120 (2025).
- [68] J. P. Dehollain, U. Mukhopadhyay, V. P. Michal, Y. Wang, B. Wunsch, C. Reichl, W. Wegscheider, M. S. Rudner, E. Demler, and L. M. K. Vandersypen, *Nagaoka ferromagnetism observed in a quantum dot plaquette*, Nature **579**, 528–533 (2020).
- [69] M. Lebrat, M. Xu, L. H. Kendrick, A. Kale, Y. Gang, P. Seetharaman, I. Morera, E. Khatami, E. Demler and, M. Greiner, *Observation of Nagaoka Polarons in a Fermi-Hubbard Quantum Simulator*, Nature **629**, 317 (2024).
- [70] P. W. Anderson, *Hidden Fermi liquid: The secret of high- T_c cuprates*, Phys. Rev. B **78**, 174505 (2008).
- [71] P. W. Anderson and P. A. Casey, *Transport anomalies of the strange metal: Resolution by hidden Fermi liquid theory*, Phys. Rev. B **80**, 094508 (2009).
- [72] P. A. Casey and P. W. Anderson, *Hidden Fermi Liquid: Self-Consistent Theory for the Normal State of High- T_c Superconductors*, Phys. Rev. Lett. **106**, 097002 (2011).
- [73] J. Krieg and P. Kopietz, *Exact renormalization group for quantum spin systems*, Phys. Rev. B **99**, 060403(R) (2019).
- [74] A. Rückriegel, D. Tarasevych, and P. Kopietz, *Phase diagram of the J_1 - J_2 quantum Heisenberg model for arbitrary spin*, Phys. Rev. B **109**, 184410 (2024).
- [75] A. Rückriegel, D. Tarasevych, J. Krieg, and P. Kopietz, *Recursive algorithm for generating high-temperature expansions for spin systems and the chiral nonlinear susceptibility*, Phys. Rev. B **110**, 144416 (2024).
- [76] T. Machado and N. Dupuis, *From local to critical fluctuations in lattice models: A nonperturbative renormalization-group approach*, Phys. Rev. E **82**, 041128 (2010).
- [77] A. Rançon and N. Dupuis, *Nonperturbative renormalization group approach to the Bose-Hubbard model*, Phys. Rev. B **83**, 172501 (2011).
- [78] A. Rançon and N. Dupuis, *Nonperturbative renormalization group approach to strongly correlated lattice bosons*, Phys. Rev. B **84**, 174513 (2011).
- [79] J. Berges, N. Tetradis, and C. Wetterich, *Non-perturbative renormalization flow in quantum field theory and statistical physics*, Phys. Rep. **363**, 223 (2002).
- [80] J. M. Pawłowski, *Aspects of the functional renormalization group*, Ann. Phys. **322**, 2831 (2007).
- [81] K. Haule, A. Rosch, J. Kroha, and P. Wölfle, *Pseudo-gaps in the t - J model: An extended dynamical mean-field theory study*, Phys. Rev. B **68**, 155119 (2003).
- [82] Y. Wang, B. Moritz, C.-C. Chen, T. P. Devereaux, and K. Wohlfeld, *Influence of magnetism and correlation on the spectral properties of doped Mott insulators*, Phys. Rev. B **97**, 115120 (2018).
- [83] J. Arnold, P. Kopietz, and A. Rückriegel, *Functional renormalization group for extremely correlated electrons*, in preparation.
- [84] A. A. Katanin, *Fulfillment of Ward identities in the functional renormalization group approach*, Phys. Rev. B **70**, 115109 (2004).
- [85] In the companion paper [83], we discuss a qualitative change in the ferromagnetic instability as function of density that might be related to the transition from partially to fully polarized ferromagnet observed in Refs. [60, 63, and 65].
- [86] K. S. D. Beach, R. J. Gooding, and F. Marsiglio, *Reliable Padé analytical continuation method based on a high-accuracy symbolic computation algorithm*, Phys. Rev. B **61**, 5147 (2000).
- [87] J. Schött, I. L. M. Locht, E. Lundin, O. Gränäs, O. Eriksson, and I. Di Marco, *Analytic continuation by averaging Padé approximants*, Phys. Rev. B **93**, 075104 (2016).
- [88] J. Kanamori, *Electron Correlation and Ferromagnetism of Transition Metals*, Prog. Theor. Phys. **30**, 275 (1963).
- [89] W. von der Linden and D. M. Edwards, *Ferromagnetism in the Hubbard model*, J. Phys.: Condens. Matter **3**, 4917 (1991).
- [90] A. Mielke, *Ferromagnetic ground states for the Hubbard model on line graphs*, J. Phys. A: Math. Gen. **24**, L73 (1991).
- [91] A. Mielke, *Ferromagnetism in the Hubbard model on line graphs and further considerations*, J. Phys. A: Math. Gen. **24**, 3311 (1991).
- [92] H. Tasaki, *Ferromagnetism in the Hubbard Model: A Constructive Approach*, Commun. Math. Phys. **242**, 445–472 (2003).
- [93] H. Hu, O. Vafek, K. Haule and, B. A. Bernevig, *Ferromagnetism vs. Antiferromagnetism in Narrow-Band Systems: Competition Between Quantum Geometry and Band Dispersion*, arXiv:2509.03575 [cond-mat.str-el] (2025).
- [94] E. Khatami, E. Perepelitsky, M. Rigol, and B. S. Shastry, *Linked-cluster expansion for the Green's function of the infinite- U Hubbard model*, Phys. Rev. E **89**, 063301 (2014).